

Monitoring present day changes in water vapour and the radiative energy balance using satellite data, reanalyses and models

Article

Published Version

EUMETSAT conference proceedings paper

Allan, R. P. ORCID: <https://orcid.org/0000-0003-0264-9447>
(2007) Monitoring present day changes in water vapour and the radiative energy balance using satellite data, reanalyses and models. Joint 2007 EUMETSAT Meteorological Satellite Conference and the 15th Satellite Meteorology & Oceanography Conference of the American Meteorological Society, P.50. ISSN 1011-3932 Available at <https://centaur.reading.ac.uk/806/>

It is advisable to refer to the publisher's version if you intend to cite from the work. See [Guidance on citing](#).

Published version at:

http://www.eumetsat.int/Home/Main/AboutEUMETSAT/Publications/ConferenceandWorkshopProceedings/2007/groups/cps/documents/document/pdf_conf_p50_s7_03_allan_v.pdf

Publisher: EUMETSAT

All outputs in CentAUR are protected by Intellectual Property Rights law, including copyright law. Copyright and IPR is retained by the creators or other copyright holders. Terms and conditions for use of this material are defined in

the [End User Agreement](#).

www.reading.ac.uk/centaur

CentAUR

Central Archive at the University of Reading

Reading's research outputs online

MONITORING PRESENT DAY CHANGES IN WATER VAPOUR AND THE RADIATIVE ENERGY BALANCE USING SATELLITE DATA, REANALYSES AND MODELS

Richard P. Allan

Environmental Systems Science Centre, University of Reading, PO Box 238, Reading, Berkshire, UK

Abstract

A combination of satellite data, reanalysis products and climate models are combined to monitor changes in water vapour, clear-sky radiative cooling of the atmosphere and precipitation over the period 1979-2006. Climate models are able to simulate observed increases in column integrated water vapour (CWV) with surface temperature (T_s) over the ocean. Changes in the observing system lead to spurious variability in water vapour and clear-sky longwave radiation in reanalysis products. Nevertheless all products considered exhibit a robust increase in clear-sky longwave radiative cooling from the atmosphere to the surface; clear-sky longwave radiative cooling of the atmosphere is found to increase with T_s at the rate of $\sim 4 \text{ Wm}^{-2} \text{ K}^{-1}$ over tropical ocean regions of mean descending vertical motion. Precipitation (P) is tightly coupled to atmospheric radiative cooling rates and this implies an increase in P with warming at a slower rate than the observed increases in CWV. Since convective precipitation depends on moisture convergence, the above implies enhanced precipitation over convective regions and reduced precipitation over convectively suppressed regimes. To quantify this response, observed and simulated changes in precipitation rate are analysed separately over regions of mean ascending and descending vertical motion over the tropics. The observed response is found to be substantially larger than the model simulations and climate change projections. It is currently not clear whether this is due to deficiencies in model parametrizations or errors in satellite retrievals.

INTRODUCTION

Projected increases in the total area affected by drought and the flood risk associated with increased frequency of heavy precipitation events are expected to exert an adverse effect on agriculture, water resources, human health and infrastructure (IPCC, 2007a, 2007b). Monitoring and understanding the present day changes in the global water cycle, including radiative feedbacks, are crucial in evaluating and improving model predictions of future climate change and its affect on society.

Observational, modelling and theoretical studies suggest that atmospheric water vapour will increase with warming at the rate of approximately 7 %/K, primarily due to the Clausius Clapeyron relationship between saturated vapour pressure and temperature (e.g. Soden et al. 2005). However, global mean precipitation changes are constrained by the atmospheric energy balance and modelling studies suggest a response of $\sim 1-3$ %/K (e.g. Held and Soden, 2006), considerably smaller than the water vapour response. These considerations suggest that convective precipitation will rise rapidly along with atmospheric moisture while away from the areas of moisture convergence, precipitation rates will diminish such that mean precipitation follows the slower increases in atmospheric cooling rates (e.g. Allen and Ingram, 2002; Trenberth et al. 2003). This implies greater extremes in precipitation (Emori and Brown, 2005) including enhanced seasonality (Chou et al. 2007), including more intense rainfall and more incidence of droughts. While there is evidence for this response (e.g. Neelin et al., 2006; Seager et al. 2007) satellite observations indicate a larger precipitation changes than the models (Wentz et al. 2007; Zhang et al. 2007).

The aim of the present study is to monitor changes in water vapour, clear-sky radiative cooling of the atmosphere and precipitation over the period 1979-2006 using a diverse range of observations, reanalysis products and climate model simulations.

METHODOLOGY AND DATA

Analysis of monthly-mean surface temperature (T_s), column integrated water vapour (CWV), surface net downward longwave radiation from the clear-sky atmosphere (SNLc), clear-sky outgoing longwave radiation to space (OLRc), clear-sky longwave radiative cooling of the atmosphere (Q_{LWc}) and precipitation rate (P) are conducted over the period 1979-2006. The tropics (30°S - 30°N) are considered in detail and 500 hPa vertical motion fields from reanalyses and the models are used to sub-sample regions of mean ascending and descending motion (Allan, 2006). Linear least squares fit regressions are calculated over the period 1980-2000.

Observations:

Observed sea surface temperature is taken from the Hadley Centre global sea Ice and Sea Surface Temperature dataset (HadISST; Rayner et al., 2003). SSM/I version 6 CWV and P data over the oceans (Wentz et al. 2007) are combined with HadISST to generate estimates of SNLc (SSM/I-OBS; Allan, 2006). A modified fit to Prata's model was also included (SSM/I-OBS-mod) which used radiometric data from four contrasting surface sites across the globe (Henderson et al. 2007). Data from the Earth Radiation Budget Satellite (ERBS; 1985-1990), Scanner for Radiation Budget satellite (ScaRaB; 1994/5) and Clouds and the Earth's Radiant Energy System (CERES; 1998 and 2000-2005) provide top of atmosphere radiative fluxes (Wielicki et al. 2002), including estimates of OLRc which were combined with observationally based SNLc to estimate Q_{LWc} . Monthly mean P from the Global Precipitation Climatology Project [GPCP; Adler et al., 2003] and from the Climate Prediction Center Merged Analysis of Precipitation [CMAP; Xie and Arkin, 1998] enhanced product (V703) were also employed for the period 1979-2006.

Reanalyses:

National Center for Environmental Prediction/National Center for Atmospheric Research reanalysis 1 (NCEP; Kalnay et al., 1996) and 24-hour forecasts from the European Centre for Medium Range Weather Forecasts 40-year reanalysis (ERA40; Uppala et al. 2005) are used to provide estimates of clear-sky radiation and water vapour. Also used are 500 hPa vertical motion fields to sub-sample regions of mean atmospheric ascent and descent.

Models:

An ensemble of atmosphere-only model simulations forced with observed sea surface temperature (AMIP3; 1979-2001) and coupled model simulations (CMIP3) from the Climate of the 20th Century runs (1950-1999) and from the SRESA1B (stabilization at 720ppm CO₂ concentration) scenario (2000-2100) were extracted from the World Climate Research Programme (WCRP) model archive at the Program for Climate Model Diagnosis and Intercomparison (PCMDI) archive (Fig. 2b). The coupled models were prescribed natural and anthropogenic forcings [for a description of the model data, see www-pcmdi.llnl.gov; Held and Soden, 2006; Emori and Brown, 2005].

INTERANNUAL VARIABILITY 1979-2006

Figure 1 shows the de-seasonalised interannual variability of column integrated water vapour (CWV), clear-sky radiation diagnostics and precipitation over the period 1979-2006 for observational estimates, reanalyses products and an ensemble of atmosphere-only climate models forced with the observed sea surface temperature (T_s). A general warming trend over the period is punctuated by large interannual fluctuations (Fig. 1a) associated with the El Niño Southern Oscillation (ENSO). This is accompanied by changes in CWV that are strongly correlated with T_s in the models and SSM/I observations (Fig.1b, Fig. 2a) with CWV increasing by around 3 mm per Kelvin increase in T_s in the SSM/I data ($\sim 8\%$ /K). Enhanced water vapour continuum emission in the atmospheric infra-red window for larger water column leads to a tight positive coupling between surface net downward longwave radiation from the clear-sky atmosphere (SNLc) and CWV (e.g. Allan, 2006) and this leads to enhanced atmospheric longwave radiative cooling to the surface for higher temperatures (Fig. 1c) at the rate of $\sim 3\text{-}4\text{ W m}^{-2}\text{K}^{-1}$ (Fig. 2c; outliers include the NCAR PCM coupled model which may be a

diagnostic error and the “SSM/I-OBS-mod” estimate which includes a modified version of the Prata (1996) algorithm used to generate SNLc (SSM/I-OBS; Henderson et al. 2007; Allan, 2006).

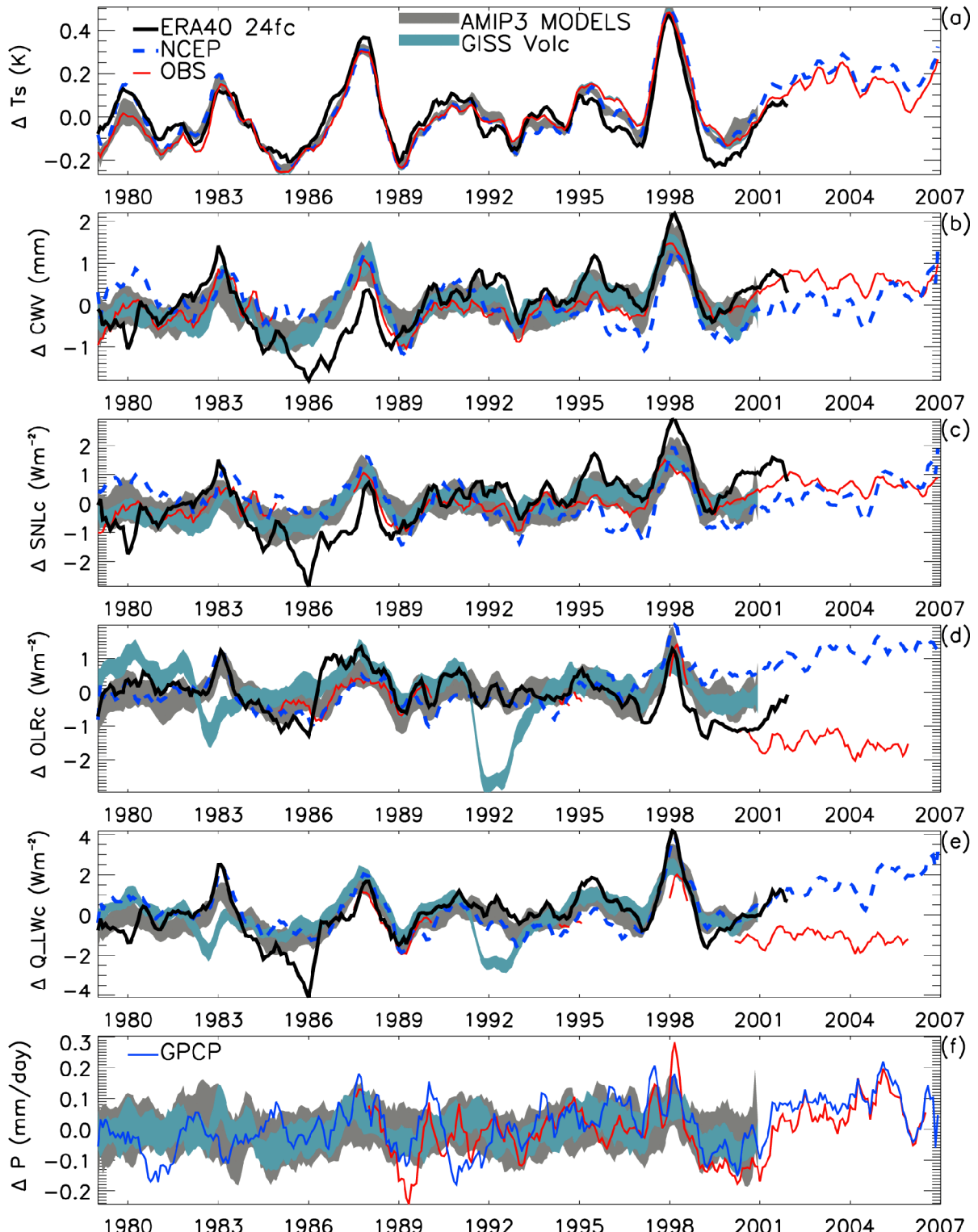


Figure 1: Deseasonalised tropical ocean anomalies of (a) surface temperature (Ts), (b) column integrated water vapour (CWV), (c) surface downward net clear-sky longwave radiation (SNLc), (d) clear-sky outgoing longwave radiation (OLRc), (e) clear-sky longwave radiative cooling of the atmosphere (Q_{LWc}) and (f) precipitation rate (P) from AMIP3 models, reanalyses and observations (HadISST in a; SSM/I in b, c and f; ERBS/ScaRaB/CERES in d; combination of a-d in e). The mean ± 1 standard deviation are shown for an ensemble of atmosphere-only climate models (grey shading); also shown are the GISS_E_R model ensembles which also include volcanic forcing.

Changes in CWV and SNLc from reanalyses (NCEP and ERA40 24-hour forecasts) are broadly similar to the model estimates but NCEP exhibits differing trends and ERA40 shows larger interannual variability. Variability of these diagnostics in reanalyses is particularly sensitive to changes in the observing system (e.g. Bengtsson et al., 2007; Allan 2007). This is also the case for estimates of clear-sky outgoing longwave radiation to space (OLRc). Observed changes in OLRc from satellite observations are also sensitive to satellite calibration and sampling issues and it is likely that the downward trend from CERES data after 2000 are spurious (e.g. Allan, 2007). Additionally, OLRc is also sensitive to volcanic aerosols as evident from the differences between the model runs with (blue) and without (grey) volcanic aerosol forcings prescribed (e.g. Allan et al. 2003) thereby making this diagnostic prone to problems for climate monitoring.

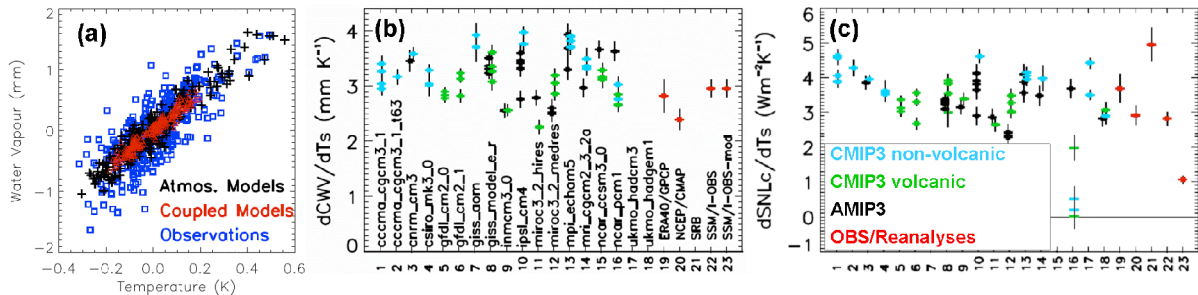


Figure 2: (a) Monthly de-seasonalised anomalies of column integrated water vapour and surface temperature over the tropical oceans in atmosphere only models forced with observed sea surface temperatures, coupled models with prescribed natural and anthropogenic radiative forcing and satellite microwave observations for the period 1979-2006; linear least squares fit for (b) column integrated water vapour (CWV) and surface temperature (Ts) and (c) surface net downward clear-sky longwave radiation (SNLc) with Ts for models, observations and reanalyses products.

However, by combining the surface and top of atmosphere clear-sky radiative fluxes, the clear-sky longwave radiative cooling of the atmosphere (Q_{LWc}) shows surprisingly good agreement between models, reanalyses and observations for much of the period (excluding the CERES observations after 2000, the Pinatubo and the El Chichon volcanic eruptions and the ERA40 data around January 1986, Fig. 1e). This is partly explained by the fact that humidity errors in the reanalyses produce compensating biases in the clear-sky longwave radiative cooling of the atmosphere at the surface and at the top of atmosphere (Allan, 2006).

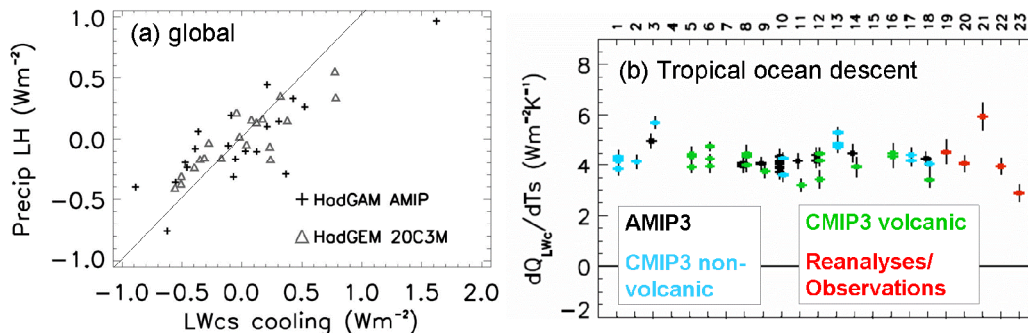


Figure 3: (a) Relationship between interannual anomalies of global mean latent heating from precipitation and clear-sky radiative cooling of the atmosphere in the Hadley Centre atmosphere-only (HadGAM) and coupled ocean-atmosphere (HadGEM) models; (b) linear sensitivity of clear-sky longwave radiative cooling of the atmosphere and surface temperature (dQ_{LWc}/dT_s) over tropical ocean regions of mean descent for models, observations and reanalyses.

Changes in precipitation rate over the tropical oceans (Fig. 1f) show large discrepancies between the GPCP or SSM/I observations and the models, and a weak dependence on Q_{LWc} , T_s and ENSO. Nevertheless, there is a strong physical basis for expecting variations in atmospheric radiative cooling to influence P (e.g. Allen and Ingram, 2002) as illustrated by the tight coupling between annual global mean P and Q_{LWc} in the Hadley Centre Global Environmental Model (HadGEM; Fig. 3a). Over the tropical ocean regions of mean descent, where radiative cooling to space is substantial, there is a robust relationship between Q_{LWc} and T_s (Fig. 3b) in the observations, reanalyses and models ($dQ_{LWc}/dT_s \sim 4 \text{ Wm}^{-2}\text{K}^{-1}$). Accounting for enhanced atmospheric solar absorption by water vapour in a warmer atmosphere, this is broadly consistent with the estimated increase in total atmospheric net radiative cooling rate with warming of $3 \text{ Wm}^{-2}\text{K}^{-1}$ (Allen and Ingram, 2002) and implies an increase in P at the rate of $\sim 3\%\text{K}^{-1}$. Precipitation changes in models and observations are now assessed in detail.

PRECIPITATION CHANGES

Figure 4 shows changes in precipitation over the period 1979-2006 for a subset of AMIP3 model simulations (model numbers 3, 8, 9, 10-12, 14-16, 18 in Fig. 2b but also including the IAP_FGOALS model) and the observations (see also, Allan and Soden, 2007). Since the behaviour of precipitation is expected to differ over the convectively active and suppressed regions of the tropics (Trenberth et al. 2003) analysis is conducted upon regions of mean ascending and descending motion separately. There are large differences between the GPCP and CMAP observations over the ascending regions (Fig. 4a). The negative trend in CMAP data before 1998 originates over the ocean (Fig. 4b) and it is likely that this is explained by changes in the observing system and spurious use of atoll data in the CMAP calibration process (Yin et al. 2004). There is good agreement between SSM/I and GPCP data over the ocean (Fig. 4b) although SSM/I data is used in both the GPCP and CMAP datasets (Yin et al. 2004). Agreement between observations is good over land (Fig. 4c), where rain gauge data is utilised, and for the descending regions (Fig. 4d-f) where a robust negative trend is evident. It is clear from Figure 4 that the model simulations appear to underestimate the response of the tropical hydrological cycle, in particular for the regions of mean descending motion.

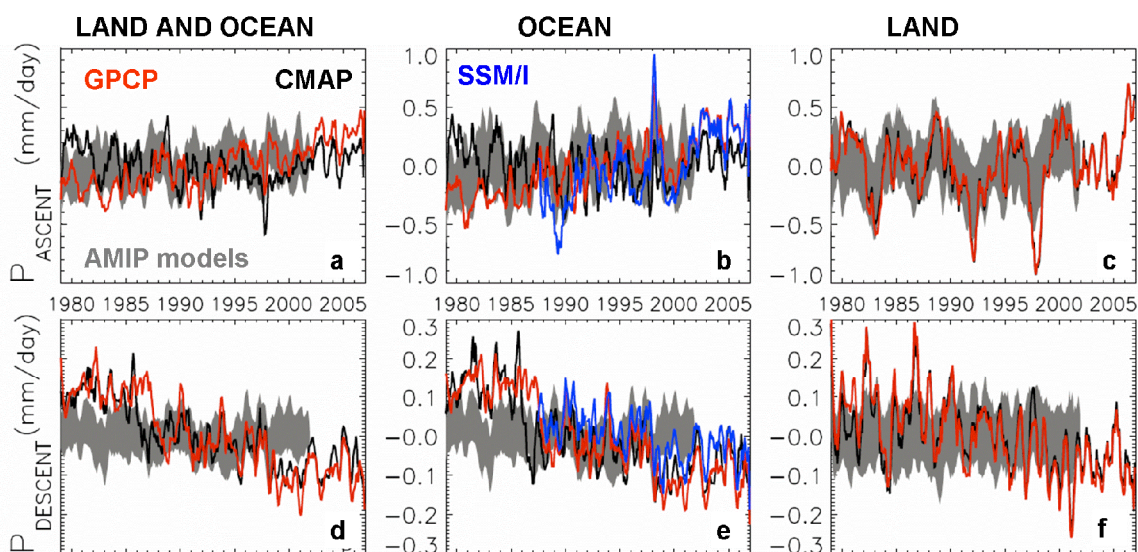


Figure 4: Deseasonalised anomalies of precipitation rate in AMIP3 models (ensemble mean ± 1 standard deviation) and observations (GPCP, CMAP, SSM/I) for regions of mean ascent (a) land and ocean, (b) ocean and (c) land and for regions of mean descending vertical motion over (d) land and ocean, (e) ocean and (f) land. 2-year averages applied.

If the models cannot reproduce the observed response of the tropical water cycle, this has implications for the accuracy of projected climate change. Changes in simulated precipitation are now analysed over the period 1950-2100 using a subset of the coupled climate models (model numbers 3-5, 7-10 and 12 in Fig. 2b but also including the IAP_FGOALS and GISS_E_H models; see also Allan and Soden, 2007). Figure 5 shows percentage changes mean P (2-year averages applied), relative to the 1979-2000 period, over the tropics and for the ascending and descending regions. Also shown are the GPCP observations.

All models show an increase in tropical mean precipitation over the period 1950-2100 although there is a large range in precipitation changes by 2100 of ~ 2 -8%. The response for the ascending regions is larger (~ 4 -12% by 2100) while the models show changes in P over the descending regions of varying sign, although predominantly negative trends. The CNRM model appears to show increased precipitation for the descending regime although this is partly explained by a step change around 2000 where the model experiments used were changed and it is possible that the mean climate of the SRESA1B differ substantially from the corresponding 20th century climate experiments for this particular model simulation.

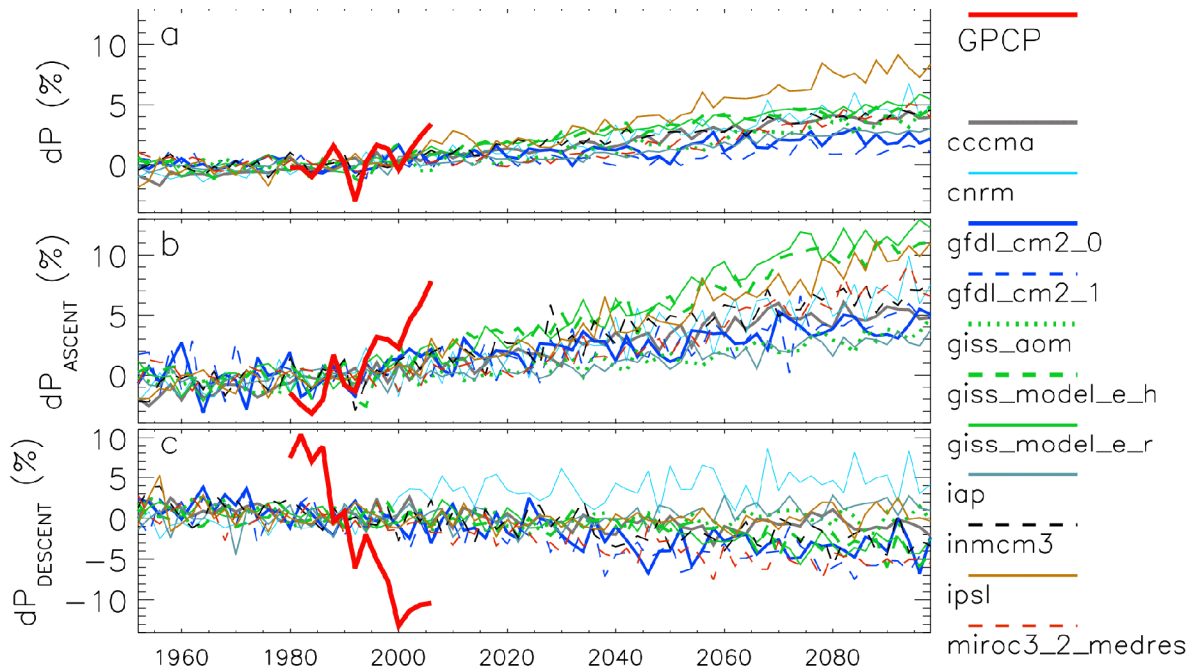


Figure 5: Percentage changes in precipitation rate (dP), relative to the 1979-2000 period, in models and GPCP observations over (a) the tropics, (b) tropical ascending regions and (c) tropical descending regions.

Trends in model ensemble mean precipitation rate are 0.3 % per decade over the period 1979-2006 and only slightly larger over the 1950-2100 period (Table 1). For a warming of ~ 0.15 K per decade over the period 1988-2006 (Allan and Soden, 2007), this translates to 2% per Kelvin warming. The GPCP trend over the 1979-2006 period is around 3 times larger than the model response although not statistically significant at the 95% confidence level. However, the observed responses over the ascending and descending tropical regimes are statistically significant and substantially larger than the model response. Over the ascending regions of the tropical circulation, the observed response is ~ 6 -7 times greater than the model response while the model simulated reduction in precipitation over the descending regions is small compared to the response calculated for the GPCP data (Table 1). Differences in absolute terms (mm/day per decade) are smaller since the mean GPCP precipitation rates are generally smaller than the model simulations (Allan and Soden, 2007).

Dataset and period	Precipitation trend (% per decade)		
	Tropics	Tropical Ascent	Tropical Descent
GPCP 1979-2006	1.07 ± 0.45	$3.66 \pm 0.48^*$	$-9.13 \pm 0.98^*$
CMIP3 1979-2006	$0.30 \pm 0.08^*$	$0.51 \pm 0.16^*$	0.00 ± 0.11
CMIP3 1950-2100	$0.35 \pm 0.01^*$	$0.58 \pm 0.02^*$	$-0.16 \pm 0.01^*$

Table 1: Trends in precipitation expressed as a percentage of the 1979-2000 mean for GPCP observations and a coupled model ensemble mean (CMIP3). * denotes correlation is significant at the 95% confidence level.

Finally, the relationships between CWV and surface temperature and precipitation and CWV are displayed in Fig. 6 for the models and observationally-based products over the tropical ascent regions. Agreement between the models and observations is good for the relationship between CWV and surface temperature, with CWV increasing at ~ 5 mm/K over oceans and ~ 3 mm/K over land. The AMIP3 and CMIP3 models simulate an increase in precipitation with CWV of ~ 0.2 to 0.25 day $^{-1}$ over land and ocean. The observations produce a slightly steeper gradient (~ 0.4 - 0.5 day $^{-1}$) although the scatter is substantial and further analysis is required to refine these estimates. Nevertheless, these relationships suggest that models underestimate the response of precipitation to changes in moisture.

CONCLUSIONS

Variability in water vapour, clear-sky radiative cooling and precipitation are analysed over the period 1979-2006 using a combination of climate models, reanalyses and observationally-based sources.

Both observations and reanalyses suffer from changes in the observing system and uncertainty relating to inter-satellite calibration and retrieval algorithms. Nevertheless, robust increases in water vapour with surface temperature can explain enhanced radiative cooling from the atmosphere to the surface over the tropics for the datasets considered. Clear-sky longwave radiative cooling of the atmosphere is found to increase by 4 Wm^{-2} per Kelvin of surface warming over tropical ocean regions of mean descending vertical motion in the models, reanalyses and observations. This enhanced cooling, offset by increased solar absorption by water vapour, imply a robust increase in tropical precipitation of around $3\%K^{-1}$, smaller than the water vapour changes which closely follow the Clausius Clapeyron relationship of around $7\%K^{-1}$ (e.g. Held and Soden, 2006)

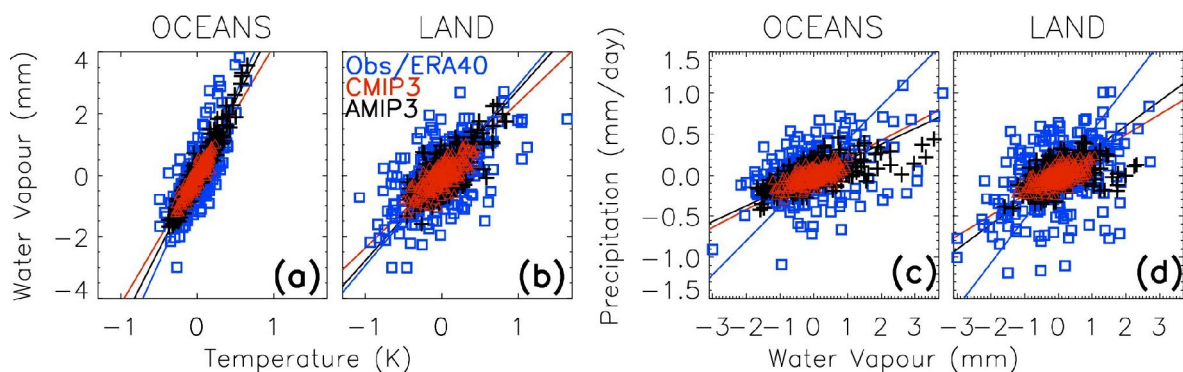


Figure 6: Scatter plots of column integrated water vapour with surface temperature for (a) ocean and (b) land and precipitation with water vapour over (c) ocean and (d) land for regions of tropical mean ascent. Monthly mean deseasonalised anomalies over the period 1980-1999 are considered for AMIP3 and CMIP3 models (model numbers 3, 8-12, 14-16 in Fig. 2b plus IAP_FGOALS). The Obs/ERA40 combination use GPCP precipitation, SMMR-SSM/I water vapour and HadSST surface temperature over the ocean and GPCP and ERA40 24 hour forecasts over land. Least squares linear fits are denoted by solid lines.

The “muted” response of precipitation compared with water vapour is simulated by models, but not apparent in the observations, consistent with previous studies (Wentz et al. 2007). Yu and Weller (2007) also note that an observationally based estimate of changes in surface latent heat flux through evaporation over the ocean is an order of magnitude larger than model simulations. This is explained through the large increases in sea-air specific humidity differences related to the Clausius Clapeyron relationship that can only be counteracted by reduced wind-stress. While reduced wind speed over land is observed (Roderick et al. 2007), over the oceans trends in wind speed are predominantly positive (Yu and Weller, 2007; Wentz et al. 2007).

The present study finds that the model simulations appear to severely underestimate the observed precipitation response in the ascending and descending branches of the tropical circulation (see also Allan and Soden, 2007). It is not yet clear whether this disparity relates to inadequacies in the model parametrizations or in the calibration and retrieval uncertainties in the satellite retrievals. It is possible that decadal fluctuations in cloud and aerosol (e.g. Wielicki et al. 2002; Ramanathan et al. 2007) and their influence on atmospheric radiative cooling and atmospheric circulation through changes in sea surface temperature gradients (Chung and Ramanathan, 2007) could influence precipitation fluctuations in the observations that make calculation of trends meaningless in the respect of projected precipitation changes. Regardless, it is vital that monitoring changes in tropical precipitation and the radiative energy balance should continue in parallel with careful assessment and improvement of the satellite datasets such that certainty in predictions of future changes in the atmospheric hydrological cycle is increased.

REFERENCES

- Allan, R.P. and B.J. Soden (2007), Large discrepancy between observed and simulated precipitation trends in the ascending and descending branches of the tropical circulation, *Geophys. Res. Lett.*, **34**, L18705, doi:10.1029/2007GL031460
- Adler, R. F., et al. (2003), The version-2 Global Precipitation Climatology Project (GPCP) monthly precipitation analysis (1979-present), *J. Hydrometeor.*, **4**, pp 1147-1167

Allan, R. P. (2006) Variability in clear-sky longwave radiative cooling of the atmosphere. *J. Geophys. Res.*, **111**(D22105), doi:10.1029/2006JD007304

Allan, R. P. (2007) Improved simulation of water vapour and clear-sky radiation using 24 hour forecasts from ERA40, *Tellus*, **59A**, pp 336-343

Allan, R. P., M. A. Ringer, and A. Slingo (2003) Evaluation of moisture in the Hadley Centre Climate Model using simulations of HIRS water vapour channel radiances, *Quarterly Journal of Royal Met. Soc.*, **129**, pp 3371-3389

Allen, M. R., and W. J. Ingram (2002) Constraints on future changes in climate and the hydrologic cycle, *Nature*, **419**, pp 224-232

Bengtsson, L., and coauthors (2007) The need for a dynamical climate reanalysis. *Bull. Amer. Meteorol. Soc.*, **88**, 4, pp 495-501

Chou, C., J. Tu, and P. Tan (2007), Asymmetry of tropical precipitation change under global warming, *Geophys. Res. Lett.*, **34**, L17708, doi:10.1029/2007GL030327.

Chung, C. E., and V. Ramanathan (2007), Relationship between trends in land precipitation and tropical SST gradient, *Geophys. Res. Lett.*, **34**, L16809, doi:10.1029/2007GL030491.

Emori, S., and S. J. Brown (2005) Dynamic and thermodynamic changes in mean and extreme precipitation under changed climate, *Geophys. Res. Lett.*, **32**(L17706), doi:10.1029/2005GL023272

Held, I. M., and B. J. Soden (2006) Robust responses of the hydrological cycle to global warming, *J. Climate.*, **19**, pp 5686-5699

Henderson, P. W., A. Slingo and S. F. Milton (2007) Evaluations of the Met Office global forecast model using ARM surface based observations. Submitted to *J. Geophys. Res.*

IPCC (2007a), *Climate Change 2007: The Physical Science Basis*. Contribution of Working Group I to the Fourth Assessment Report of the Intergovernmental Panel on Climate Change, 996 pp., Cambridge University Press, Cambridge, United Kingdom and New York, NY, USA.

IPCC (2007b), *Climate Change 2007: Impacts, Adaptation and Vulnerability*. Working Group II Contribution to the Inter-governmental Panel on Climate Change Fourth Assessment Report, Summary for Policy Makers, 23 pp.

Kalnay, E., et al. (1996) The NCEP/NCAR 40-year reanalysis project, *Bull. Amer. Met. Soc.*, **77**, pp 437-471.

Neelin, J. D., M. Munnich, H. Su, J. E. Meyerson, and C. E. Holloway (2006) Tropical drying trends in global warming models and observations, *PNAS*, **103**(16), pp 6110-6115

Prata, A. J. (1996) A new longwave formula for estimating downwelling clear sky radiation at the surface. *Q. J. R. Meteorol. Soc.*, **122**, pp 1127-1151

Ramanathan, V., M. V. Ramana, G. Roberts, D. Kim, C. Corrigan, C. Chung and D. Winker (2007) Warming trends in Asia amplified by brown cloud solar absorption. *Nature* **448**, pp 575-578

Roderick, M. L., L. D. Rotstayn, G. Farquhar, and M. Hobbins (2007), On the attribution of changing pan evaporation, *Geophys. Res. Lett.*, **34**, L17403, doi:10.1029/2007GL031166.

Seager, R., et al. (2007) Model Projections of an Imminent Transition to a More Arid Climate in Southwestern North America, *Science*, **316**(5828), pp 1181-1184

Soden, B. J., D. L. Jackson, V. Ramaswamy, M. D. Schwarzkopf, and X. Huang (2005) The radiative signature of upper tropospheric moistening, *Science*, **310**, pp 841-844.

Trenberth, K. E., A. Dai, R. M. Rasmussen, and D. B. Parsons (2003) The changing character of precipitation, *Bull. Amer. Met. Soc.*, **84**, pp 1205-1217

Uppala, S. M., et al. (2005) The ERA-40 re-analysis, *Quart. J. Roy. Meteorol. Soc.*, **131**, 2961-3012

Wentz, F. J., L. Ricciardulli, K. Hilburn, and C. Mears (2007) How much more rain will global warming bring?, *Science*, **317**, pp 233-235.

Wielicki, B. A., et al. (2002) Evidence for large decadal variability in the tropical mean radiative energy budget, *Science*, **295**, pp 841-844

Xie, P., and P. A. Arkin (1998) Global monthly precipitation estimates from satellite-observed outgoing longwave radiation, *J. Climate*, **11**, pp 137-164

Yin, X., A. Gruber, and P. Arkin (2004), Comparison of the GPCP and CMAP merged gauge-satellite monthly precipitation products for the period 1979-2001, *J. Hydromet.*, **5**, pp 1207-1222

Yu, L. and R. A. Weller (2007) Objectively analyzed air-sea heat fluxes for the global ice-free oceans (1981-2005). *Bull. Americ. Meteorol. Soc.*, **88**, 4, pp 527-539

Zhang, X., et al. (2007) Detection of human influence on twentieth-century precipitation trends. *Nature*, **448**, pp 461-465